DOI: 10.1002/jmor.21699

RESEARCH ARTICLE



Tradeoffs between bite force and gape in Eulemur and Varecia

Myra F. Laird¹ | Taylor A. Polvadore² | Gabrielle A. Hirschkorn³ |

Julie C. McKinney³ | Callum F. Ross⁴ | Andrea B. Taylor⁵ | Claire E. Terhune² |

Jose Iriarte-Diaz⁶ |

Correspondence

Myra F. Laird, Department of Basic and Translational Sciences, University of Pennsylvania, Levy 443, 4010 Locust Street Philadelphia, PA 19104, USA. Email: mflaird@upenn.edu

Funding information

National Science Foundation, Grant/Award Numbers: BCS-1945771, BCS-1944915, BCS-1945283, BCS-1945767, BCS 0924592, 0452160; University of Southern California

Abstract

In 1974, Sue Herring described the relationship between two important performance variables in the feeding system, bite force and gape. These variables are inversely related, such that, without specific muscular adaptations, most animals cannot produce high bite forces at large gapes for a given sized muscle. Despite the importance of these variables for feeding biomechanics and functional ecology, the paucity of in vivo bite force data in primates has led to bite forces largely being estimated through ex vivo methods. Here, we quantify and compare in vivo bite forces and gapes with output from simulated musculoskeletal models in two craniofacially distinct strepsirrhines: Eulemur, which has a shorter jaw and slower chewing cycle durations relative to jaw length and body mass compared to Varecia. Bite forces were collected across a range of linear gapes from 16 adult lemurs (suborder Strepsirrhini) at the Duke Lemur Center in Durham, North Carolina representing three species: Eulemur flavifrons (n = 6; 3F, 3M), Varecia variegata (n = 5; 3F, 2M), and Varecia rubra (n = 5; 5F). Maximum linear and angular gapes were significantly higher for Varecia compared to Eulemur (p = .01) but there were no significant differences in recorded maximum in vivo bite forces (p = .88). Simulated muscle models using architectural data for these taxa suggest this approach is an accurate method of estimating bite force-gape tradeoffs in addition to variables such as fiber length, fiber operating range, and gapes associated with maximum force. Our in vivo and modeling data suggest Varecia has reduced bite force capacities in favor of absolutely wider gapes compared to Eulemur in relation to their longer jaws. Importantly, our comparisons validate the simulated muscle approach for estimating bite force as a function of gape in extant and fossil primates.

KEYWORDS

craniofacial, muscle, musculoskeletal model, strepsirrhine

This is an open access article under the terms of the Creative Commons Attribution-NonCommercial-NoDerivs License, which permits use and distribution in any medium, provided the original work is properly cited, the use is non-commercial and no modifications or adaptations are made.

© 2024 The Authors. *Journal of Morphology* published by Wiley Periodicals LLC.

¹Department of Basic and Translational Sciences, School of Dental Medicine, University of Pennsylvania, Philadelphia, Pennsylvania, USA

²Department of Anthropology, University of Arkansas, Fayetteville, Arkansas, USA

³Duke Lemur Center, Duke University, Durham, North Carolina, USA

⁴Department of Organismal Biology and Anatomy, University of Chicago, Chicago, Illinois, USA

⁵Department of Foundational Biomedical Sciences, Touro University, Vallejo, California, USA

⁶Department of Biology, University of the South, Sewanee, Tennessee, USA

/doi/10.1002/jmor.21699 by University Of Pennsylvania

Library on [19/07/2024]. See the

for rules of

.0974687, 2024, 5, Downloaded

1 | INTRODUCTION

Sue Herring's 1974 paper, "The superficial masseter and gape in mammals," describes the theoretical effect of muscle stretch on force output in the masseter muscle (Herring & Herring, 1974) and lays the groundwork for subsequent experimental and theoretical work modeling bite forces and jaw muscle function (Dumont & Herrel, 2003; van Eijden & Turkawski, 2001; Eng et al., 2009; Iriarte-Diaz et al., 2017; Lindauer et al., 1993; Santana, 2016; Williams et al., 2009). Bite force and gape, two key performance metrics of the feeding system, are inversely related such that, for a given muscle size, fibers generate maximum force at an optimal length, and muscle fibers operating at lengths shorter or longer than their optimum result in reduced muscle and bite forces. Without specific muscular adaptations for high bite forces at wide gapes, large, mechanically challenging foods impose a constraint on feeding system performance as these foods require the jaw muscles to operate outside of their presumed optimum. Following the publication of Herring and Herring (1974), bite force-gape tradeoffs have been experimentally validated in numerous taxa (Dumont & Herrel, 2003; van Eijden & Turkawski, 2001; Eng et al., 2009; Lindauer et al., 1993; Williams et al., 2009; Zablocki Thomas et al., 2018). However, despite the importance of bite force and gape in understanding feeding system form and function, there are few in vivo studies examining these performance metrics in nonhuman primates (humans, macaques, mouse lemurs, marmosets, and capuchins; Chazeau et al., 2013; Dechow & Carlson, 1983; Hylander, 1977; Laird et al., 2023b; Thomas et al., 2015; Vinyard et al., 2009). Muscle simulation provides an alternative approach to estimating variation in bite force-gape tradeoffs (Iriarte-Diaz et al., 2017). Muscle simulation provides a method for estimating bite force and gape in addition to muscle strain and fiber architecture dynamics in species and muscles that are not typically available for experimental approaches. However, output from in vivo and muscle simulation approaches to bite force and gape have not been compared in primates. Here, we directly compare these measures for two strepsirrhine genera that vary in craniofacial morphology-Eulemur and Varecia-and discuss the implications of these results for studies of feeding system performance in extant and fossil primates.

The relationship between bite force and gape ultimately results from the combination of both muscular and geometric variables in the feeding system. Muscular determinants of bite force include their static and dynamic architecture, specific tension, activation patterns, and fiber phenotype (e.g., Anapol & Herring, 1989; Dechow & Carlson, 1990; Gans & Bock, 1965; Laird et al., 2020, 2023a; Powell et al., 1984; Taylor et al., 2009, 2019; Holmes & Taylor, 2021; Wall et al., 2013). Geometric considerations include jaw length, the positioning of the muscles within the facial skeleton, and the location of bite force on the toothrow. Following a constrained lever model of the mandible, bite forces increase posteriorly on the toothrow until the first or second molar, after which bite forces decrease with the distal-most molars (Edmonds & Glowacka, 2020; Greaves, 1978;

1975; Radinsky, 1981; 2018; Hvlander. Ross et Spencer, 1998, 1999; Thompson et al., 2003). Primates that maximize bite force tend to have shorter jaws, greater jaw-muscle mechanical advantage and smaller canines, and often have shorter, pinnatefibered muscles with greater physiological cross-sectional area (PCSA) (Perry et al., 2011a; Wright, 2005; but see Taylor & Vinyard, 2009). By contrast, species favoring wide gapes typically have longer jaws, reduced jaw muscle mechanical advantage, and muscles with longer, less pinnate fibers that facilitate muscle stretch (Herring & Herring, 1974; Smith, 1984; Taylor et al., 2009; Terhune et al., 2015). However, some primates have specific muscular adaptations to circumvent the expected tradeoff between bite force and gape. Large PCSAs in tufted capuchins (Sapajus apella), for example, are achieved through increased muscle mass rather than changing fiber length or pinnation angle, which facilitates larger bite forces at wide gapes compared to untufted capuchins (Taylor & Vinyard, 2009). Common marmosets (Callithrix jacchus) adopt a slightly different strategy by reducing sarcomere operating ranges to minimize muscle stretch, enabling them to optimize bite force at the gapes at which they gouge trees (Eng et al., 2009; Vinyard et al., 2003).

Musculoskeletal models, defined as "computational representations of bone geometries, joint morphologies, musculotendon unit (MTU) attachments and force-generating properties" (Charles et al., 2022, p1644), are a common approach to assess muscle function, particularly in the locomotor system (e.g., Anderson & Pandy, 2003; Delp et al., 2007; Hill, 1938, 1950; Peterson et al., 2011; Thelen, 2003). Validation of these models using in vivo data from locomotor muscles suggests they are accurate in predicting forcelength and force-velocity tradeoffs, particularly if the models allow for the independent recruitment of fast and slow motor units (Biewener et al., 2014; van Ingen Schenau et al., 1988; Lee et al., 2013; Perreault et al., 2003; Sandercock & Heckman, 1997; Wakeling et al., 2012). However, the use of musculoskeletal models in the feeding system is less common (but see Koolstra & Van Eijden, 2001; Taverne et al., 2000; Xu et al., 2008). Previous use of these models in the human feeding system has been limited but includes testing the forces relating to mandibular distraction osteogenesis (de Zee et al., 2007). Gröning et al. (2013) assessed the accuracy of multibody dynamics models compared to in vivo measurements in a lizard (Tupinambis merianae) finding the models predicted bite force accurately but were sensitive to changes in muscle architecture data such as fiber length and muscle stress. Within non-human primates, musculoskeletal models have been used in multibody models of the macaque feeding muscles (Curtis et al., 2008; Shi et al., 2012).

One limitation to the use of musculoskeletal models in the primate feeding system is that these models are highly sensitive to accurate values for muscle architecture data (such as fiber length and pinnation angles) but also to physiological muscle parameters (such as the location of the optimal muscle fiber length, $L_{\rm f,0}$). Muscle architecture data can be obtained directly from dissections, but physiological muscle parameters are harder to experimentally measure in non-human primates (but see Laird et al., 2020, 2023a)

and appropriate selection of these model parameters requires validation from in vivo data. In vivo bite forces have only been published for a select few primates (e.g., Chazeau et al., 2013; Dechow & Carlson, 1990; Hylander, 1979; Thomas et al., 2015; Vinyard et al., 2009; Zablocki Thomas et al., 2018), and the impact of gape on bite force has only recently been empirically demonstrated in tufted capuchins (Laird et al., 2023b). Similarly, in vivo maximum gape data have been collected in sedated catarrhines (Hylander, 2013), and estimated in select species using maximum ingested food size (Paciulli et al., 2020; Perry & Hartstone-Rose, 2010; Perry et al., 2015). As a result, primate multibody analyses using musculoskeletal models have relied on accurate muscle architecture data but had to make assumptions about muscle dynamics that are as yet unverified (Curtis et al., 2008; Shi et al., 2012). Muscle architecture force and excursion estimates assume maximal contraction of the muscle, which is unlikely to occur during routine feeding or aggression, although in vivo bite forces were similar to modeled bite forces from PCSA data in bats (Herrel et al., 2008). Without experimentally recorded bite force data, it is difficult to assess how well a musculoskeletal model predicts actual muscle function. Here, we compare bite forces and gapes from in vivo data collection and musculoskeletal models for the jaw adductors for two strepsirrhines-Eulemur and Varecia.

Eulemur and Varecia are relatively closely related lemurids, but these genera differ in body size, craniofacial morphology, and chewing rate (Table 1). Mean body mass of *E. flavifrons* is estimated as 2.12 kg compared to 3.5 kg in *V. rubra* and 3.57 kg in *V. variegata* (Dickinson et al., 2022; Hartstone-Rose & Perry, 2011; Perry et al., 2011a), and mean jaw length in *E. flavifrons* is 59.5 mm compared to 74.6–75.1 mm in *V. rubra* (Perry et al., 2011a). Eulemur also have longer chewing cycle duration relative to their body mass and jaw length compared to *Varecia* (Ross et al., 2009). Muscle architecture data indicate *Varecia* have absolutely larger muscle masses and longer fibers compared to *Eulemur*. Summed PCSA for

Varecia is larger than Eulemur (Table 1); however, PCSA values for the three largest jaw adductors (superficial masseter, temporalis, and medial pterygoid) are only slightly higher in Varecia. These muscle architecture data combined with craniodental morphology were used to estimate bite forces on the postcanine dentition suggesting V. rubra should have larger bite forces compared to E. flavifrons (Perry et al., 2011b). Gape differences calculated from maximum ingested food size and craniodental morphology indicate V. rubra should have larger gapes compared to E. flavifrons (Fricano & Perry, 2019; Perry et al., 2011a). Based on these previous studies, we predict Varecia will have larger bite force and gape than Eulemur. We test the following three hypotheses:

Hypothesis 1. Varecia has larger in vivo bite force and gape than Eulemur.

Published estimates of body mass, jaw length, adductor muscle mass, adductor fiber lengths, PCSA, bony gape angle, bony linear incisive gape, maximum ingested food size, and architecturally derived posterior bite force are larger in *Varecia* compared to *Eulemur* (Table 1). In vivo measures of bite force and gape are, therefore, expected to be absolutely larger in *Varecia* compared to *Eulemur*. Additionally, we predict no differences in in vivo bite force or gape between *V. variegata* and *V. rubra*.

Hypothesis 2. *Eulemur* and *Varecia* simulated muscle bite forces and gapes do not differ from in vivo measures (H1), with *Varecia* having larger simulated bite force and gape compared to *Eulemur*.

Here, we use musculoskeletal models to simulate bite force and gape in *Eulemur* and *Varecia*. If the model can predict the observed in vivo forces and gapes and their relationship, we expect the simulated

TABLE 1 Published muscle, bite force, and gape estimates for Eulemur flavifrons and Varecia rubra.

Measure	Eulemur flavifrons	Varecia rubra	Genus comparison	Reference
Body mass (kg)	2.12	3.5	V > E	Dickinson et al. (2022); Hartstone-Rose and Perry (2011); Perry et al. (2011a)
Jaw length (mm)	59.5	74.6-75.1	V > E	Perry et al. (2011a)
Muscle mass (g)	7.47	11.9	V > E	Perry et al. (2011a)
Fiber length (mm)	9.2	11.4	V > E	Perry et al. (2011a)
Summed PCSA (cm ²)	7.67	9.53	V > E	Perry et al. (2011a)
Gape angle (deg)	42.76	50.48	V > E	Fricano and Perry (2019)
Linear incisive gape (mm)	46.03	57.2	V > E	Fricano and Perry (2019)
Posterior bite force (N)	44.9	69.55	V > E	Perry et al. (2011b)
Maximum ingested food size (cm ³)	19.7	54.95	V > E	Perry and Hartstone-Rose (2010)
Chew cycle duration (s)	0.32 ^a	0.32	V = E	Ross et al. (2009)

Note: All muscle architecture measures are summed for the jaw adductors. Summed physiological cross-sectional area (PCSA) values include the deep and superficial masseter, deep and superficial temporalis, medial pterygoid, zygomatico-mandibularis, and zygomatic temporalis (Perry et al., 2011a, 2011b). ^aChew cycle duration is for *Eulemur fulvus* since *E. flavifrons* was not available (Ross et al., 2009).

.0974687, 2024, 5, Downloaded from https://onlinelibrary.wiley.com/doi/10.1002/jmor.21699 by University Of Pennsylvania, Wiley Online Library on [19/07/2024]. See the Terms

on Wiley Online Library for rules of

results to be the same as Hypothesis 1. However, model output is

expected to vary with muscle architecture parameters, and we expect modeled bite force magnitude and the relationship between bite force and gape to vary when using different sets of muscle architecture data. Overall, Varecia is expected to have larger simulated bite force and gape compared to Eulemur, and we expect no differences in either variable between V. variegata and V. rubra.

Hypothesis 3. Model output for peak bite force and muscle operating ranges are larger in Varecia compared to Eulemur.

Model output for muscle variables not available from the in vivo data are expected to reflect differences in bite force and gape between Eulemur and Varecia detailed in Hypothesis 1. Peak bite force and muscle operating ranges are expected to be larger in Varecia consistent with their expectation of larger in vivo bite force and gape.

MATERIALS AND METHODS

In vivo bite forces and linear gapes were collected from 16 adult lemurs over a 4-week period in 2022 at the Duke Lemur Center in Durham, North Carolina (Table 2). Data were collected from three species: Eulemur flavifrons (n = 6; 3F, 3M), Varecia variegata (n = 5; 3F, 2M), and Varecia rubra (n = 5; 5F). All experiments were reviewed and approved by Institutional Animal Care and Use Committees at the

University of Southern California #21241, the University of Pennsylvania #807395, and Duke University #A186-20-09, and were performed in accordance with relevant guidelines and regulations.

2.1 In vivo data collection and analyses

A total of 1139 bites were collected from the 16 animals in 5-mm increments of linear gape beginning at 10 mm until the animal was no longer willing to bite (Table 2). All analyses were conducted on bite force and gape values recorded on the postcanine dentition. At least 30 bites were obtained for each animal, and the highest bite force at each gape was retained for the analyses representing a minimum estimate of maximum bite force. Bite forces were collected using a custom-built bite force transducer based on a model described by Herrel and colleagues (e.g., Herrel et al., 1999; Aguirre et al., 2003; Herrel et al., 2001, 2004, 2005; Verwaijen et al., 2002). Briefly, the animal bites on the ends of two metal plates fixed to a compressive piezoelectric load cell (Kistler 9203, maximum capacity of 500 N). The metal plates were wrapped in cushioned athletic tape to protect the animal's teeth, and the animals were trained to bite on the plates for a few days before data recording (Figure 1). The spacing between the bite plates-gape distance (mm)-was controlled by an adjustable micrometer (Mitutoyo 152-103). Output from the load cell was amplified (Kistler handheld amplifier-5995A) and passed through an analog-to-digital converter (Adafruit Industries ADS1115) to a

Sample composition, age (in years) at time of data collection, the number of bites recorded from each animal, maximum recorded bite force, and recorded linear gape range.

Animal number	Species	Sex	Age (y)	Number of bites	Maximum bite force (N)	Linear gape range (mm)
7140	E. flavifrons	М	9.5	59	203.46	10-30
7271	E. flavifrons	М	10	122	184.68	10-20
6970	E. flavifrons	F	12.5	30	187.20	10-30
6969	E. flavifrons	М	12.5	37	153.85	10-30
7272	E. flavifrons	F	8	70	109.91	10-25
7180	E. flavifrons	F	8.4	47	159.66	10-35
7278	V. rubra	М	5.3	64	189.84	10-30
7298	V. rubra	F	4.3	74	136.48	10-30
7251	V. rubra	М	6.2	91	131.95	10-45
7297	V. rubra	F	4.3	79	179.72	10-30
7389	V. rubra	F	4.3	62	188.23	10-35
7154	V. variegata	F	9.3	90	154.30	10-45
7295	V. variegata	F	4.3	84	109.45	10-45
7296	V. variegata	F	4.3	49	188.12	10-45
7287	V. variegata	F	6.6	101	171.12	10-45
6917	V. variegata	F	17.5	80	191.71	10-35

FIGURE 1 Eulemur flavifrons (#6969, male) voluntarily biting the force transducer for yogurt reward in his home enclosure at the Duke Lemur Center, Durham, North Carolina. Photo by Gabrielle Hirschkorn.

Raspberry Pi 4 Model B where data collection was controlled using custom Python code. Biting was incentivized by a liquid reward administered through a plastic cannula attached to the underside of the top bite plate. The liquid reward consisted of watered-down yogurt, peanut butter, or sweet potato baby food depending on individual preference. All bites were monitored, and reward was typically withheld if the animal did not exceed the force used on their previous bites; this incentivized the animals to bite using higher forces. Additional reward was given for bites following a gape change or if the animal became visibly frustrated or lost interest in biting.

Separate experiments were conducted to calculate a calibration factor between the amplified output values and Newtons of force. The bite plates were statically loaded three times with 100, 200, and 500 g weights at 10, 15, and 20 mm gape inclusive of the bite plates. For each weight, these data suggested there were no significant differences in amplified force values between gapes, and a standard corrective factor could be applied to convert amplified forces to Newtons.

In addition to in vivo bite forces and gapes, linear gape was opportunistically obtained from one *V. variegata* (#7154) under sedation for reasons unrelated to this study following procedures in Hylander (2013).

Linear gapes were converted to angular gapes using jaw lengths from species-sex matched 3D models (detailed below).

All analyses of the in vivo data were conducted in R v. 3.6.2 (R core team, 2023) using the "ggplot2," "ggsci," and "readxl" packages (Wickham, 2016; Wickham & Bryan, 2022; Xiao, 2018). Differences

between the taxa in maximum bite force, linear gape, and angular gape for each animal were tested using Kruskal–Wallis tests with significance set at α < .05.

To quantify differences in curvature shape around peak bite force across animals, custom R code was written to calculate the radius of curvature fit across three bite force-gape points. The first point was the gape at maximum bite force and the other two were the maximum bite forces for gapes on either side of the first point's gape. The radius of curvature calculation fits a circle to this series of points and measures the radius of the circle; wider curves have a larger radius of curvature. Differences in radius of curvature between *Eulemur* and *Varecia* were tested using a Kruskal–Wallis test.

2.2 | Muscle architecture

Muscle architecture data were recorded from the superficial masseter, medial pterygoid, and temporalis from one cadaveric adult Eulemur flavifrons from the Duke Lemur Center and one Varecia rubra from the cleveland museum of natural history, both of unknown sex, following a combination of published protocols (Antón, 1999, 2000; Perry et al., 2011a; Taylor et al., 2009; Terhune et al., 2015; Table 3). Muscles were first dissected from the skull, blotted, and trimmed of excess fat and fascia. The masseter muscle was separated into superficial and deep sections. All muscles were weighed to the nearest 0.001 g. Muscles were then separately digested in 30% nitric acid until individual fiber bundles were able to be separated from their proximal and distal myotendinous junctions and mounted on slides for measurement. Fibers were selected from the anterior and posterior portions of the temporalis; fibers from the superficial masseter and medial pterygoid were selected from a variety of locations across the muscle to capture variation in fiber length within each muscle. Mounted fibers were then used to measure average fiber length (L_f) , where 20-25 fibers were measured (in mm) from a given section or muscle. Pinnation angles were not measured for these muscles (following Lieber, 2022); however, pinnation angles reported in Perry et al. (2011a) were included in models. PCSA for each muscle was calculated using average L_f as:

PCSA(cm²) = muscle mass/ $(L_f/10) \times 1.0564$ gm/cm³,

with the later constant representing an estimate of the specific density of muscle (Murphy & Beardsley, 1974; Table 3).

2.3 | Creation of virtual bone and muscle segment models

Virtual 3D muscle models of the crania and mandibles were created to simulate the effect of gape on bite force capabilities. We created four different 3D models to match the in vivo bite force collected (one male and one female *E. flavifrons*, one female *V. rubra*, and one female *V. variegata*). A 3D skull scan was not

.0974687, 2024, 5, Downloaded

//onlinelibrary.wiley.com/doi/10.1002/jmor.21699 by University Of Pennsylvania, Wiley Online Library on [19/07/2024]. See the Terms

ns) on Wiley Online Library for rules of use; OA

Musele diefineetale parameters used for modeling.									
	Eulemur f This	Perry et al.	Varecia ru This	<i>ıbra</i> Perry et al.					
	study	(2011) ^a	study	(2011) ^a					
	n = 1	n = 1	n = 1	n = 2					
Superficial masseter									
Jaw length (mm)	73	59.5	71.94	74.85					
Mass (g)	1.336	1.79	1.566	2.8					
Lf (mm)	10.984	8.1	10.637	11.05					
pinn (degrees)	n/a	12	n/a	10.5					
PCSA (cm ²) ^a	1.151	1.9	1.394	2.4					
Temporalis									
Mass (g)	2.766	4.01	3.738	5.99					
Lf (mm)	9.595	10.95	11.888	13.3					
pinn (degrees)	n/a	12.52	n/a	11.5					
PCSA (cm ²) ^a	2.729	3.31	2.976	3.99					
Medial pterygoid									
Mass (g)	0.618	0.81	0.715	1.1					
Lf (mm)	6.996	6.8	10.244	8.4					
pinn (degrees)	n/a	22	n/a	12					
PCSA (cm ²) ^a	0.836	1.13	0.661	1.25					

^aOur definition of the superficial masseter is equivalent to Perry et al.'s (2011a) superficial and deep masseter, and our temporalis is equivalent to their superficial and deep temporalis. For muscle mass and physiological cross-sectional area (PCSA), we summed their values for these individual parts, and for their fiber lengths and pinnation we took an average across all parts.

available for male V. rubra, and we were not able to collect in vivo data for male V. variegata. The 3D skull scans for all strepsirrhines in this study were available in online repositories (see Table \$1). Modeled muscles were virtually manipulated to mimic different gapes and the effects of muscle position, orientation, and relative length, and to calculate bite force at particular bite points. Virtual muscle segments were generated using custom MATLAB scripts previously described (Iriarte-Diaz et al., 2017). Briefly, the muscle attachments of the temporalis, superficial masseter, and medial pterygoid are mapped onto both the cranium and the mandible. Each muscle is divided into a series of anterior to posterior equidistant muscle segments and the attachment points for each segment are calculated. A muscle segment, representing a MTU, is then calculated by connecting the cranial and mandibular attachment points and wrapping the bone surface (Figure 2a). The origin and the direction of the segment was determined as a straight line that connects the points where the muscle starts to wrap each bone. Finally, to match the model to the muscle architecture data, the bone and muscle models were scaled so that the mandible model has the same length as reported in Table 3.

2.4 | Calculation of muscle force and bite force

Because the effect of gape on bite force is expected to differ between anterior and posterior muscles fibers, bite force was first calculated for each individual muscle segment, and the individual muscles segments were then summed to calculate the total bite force. Bite force (F^{Bite}) produced by individual muscle segments was estimated using the following equation:

$$F^{Bite} = \frac{2 \times F_{(gape)}^{Max} \times d^{Segment}}{d^{Bite}},$$
 (1)

where $F_{(gape)}^{Max}$ is the maximum force generated by an individual muscle segment at a given gape multiplied by two to simulate the effect of left and right side muscles, $d^{Segment}$ is the moment arm (i.e., the perpendicular distance of the jaw joint) of the individual muscle segment, and d^{Bite} is the distance of the bite point to the jaw joint (Figure 2b). The maximum force generated by a muscle segment, $F_{(gape)}^{Max}$, was calculated as

$$F_{(gape)}^{Max} = F^{Max} \times \left(F_{active}^{Rel} + F_{passive}^{Rel} \right),$$
 (2)

where F^{max} is the maximum tetanic force that the muscle segment can generate, F^{Rel}_{active} and $F^{Rel}_{passive}$ are the relative active and passive force that the muscle segment can produce from a normalized fiber length-force curve (Figure 3, Millard et al., 2013). The maximum tetanic force of a single muscle segment, F^{max} , was calculated as the maximum tetanic force for the whole muscle divided by the number of muscle segments modeled as

$$F^{Max} = \frac{\sigma \times PCSA \times \cos \alpha}{number \ of \ segments},$$
 (3)

where σ is the specific tension of skeletal muscle (estimated to be ~30 N/cm² for a homogeneously IIM muscle), PCSA is the physiological cross-sectional area of the muscle (in cm²; either from our specimens or Perry et al., 2011a) and α is the pinnation angle (in degrees; from Perry et al., 2011a in all models).

Finally, to determine F_{active}^{Rel} and $F_{passive}^{Rel}$ we needed to estimate the relative change in muscle fiber length (i.e., muscle fiber strain, ε_f) as a function of changes in the MTU length, which depends on the architecture of the muscle. For example, in parallel muscles, where muscle fibers are oriented parallel to the muscle's line of action, fiber strain is expected to be proportional to changes in the length of the whole muscle (Azizi & Deslauriers, 2014). In contrast, in pinnate muscles, where muscle fibers are arranged at an angle relative to the muscle's line of action, the relationship between muscle fiber strain (ε_f) and whole muscle length change depends on the pinnation angle (α) (Figure 4). To predict the effect of length changes of the whole muscle on muscle fiber strain, we used a simple geometric muscle model where we assumed that all muscle fibers are straight, parallel, of equal length, and coplanar (Figure 4, Azizi & Deslauriers, 2014; Dick & Wakeling, 2018). In this model, we also assumed that as the muscle changes length, the pinnation angle (α; from Perry

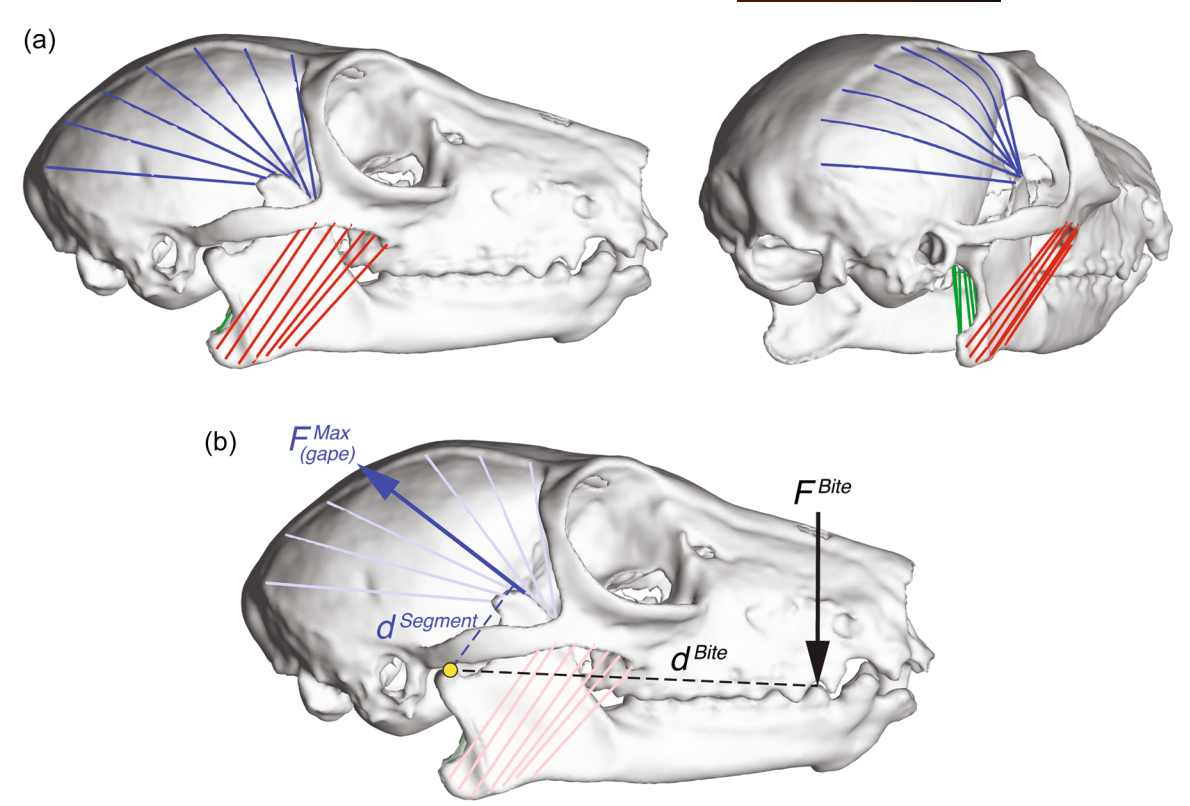


FIGURE 2 Examples of muscle segments and biomechanical parameters calculated. (a) Model of Eulemur in lateral and posterolateral views showing the location of the three modeled muscles: temporalis (blue), superficial masseter (red), and medial pterygoid (green). Each line indicates a muscle segment that represents a muscle-tendon unit (MTU). (b) Diagram showing the biomechanical parameters calculated in this study on a temporalis muscle segment. For each muscle segment, we calculated the maximum force generated for a given gape ($F_{\text{gape}}^{(gape)}$), the moment arm of the muscle segment force (d^{Segment}) as perpendicular distance of the muscle force vector to the TMJ axis (yellow dot), the bite force (F^{Bite}) as the resultant force at the bite point, and the moment arm of the bite force (d^{Bite}) as the perpendicular distance of the bite point to the TMJ axis. Note that because not all muscle segments are modeled as straight lines (such as the temporalis), the direction of the muscle force segment was estimated as the direction of the segment near its attachment point on the mandible.

et al., 2011a) varies as the muscle thickness (h) remains constant. Based on this model, we can estimate the muscle fiber strain (ε_f) as:

$$\varepsilon_{\rm f} = 1 - \sqrt{\frac{(L_{\rm f,occ} \sin \alpha)^2 + (L_{\rm f,occ} \cos \alpha + \Delta m)^2}{L_{\rm f,occ}^2}},$$
 (4)

where $L_{f,occ}$ is the muscle fiber length at occlusion and Δm is the difference is muscle segment length, calculated from the simulated gapes of the 3D bone and muscle models. We then determined the normalized fiber length as $L_{\rm f,occ}/L_{\rm f,0}$ + $\epsilon_{\rm f}$, where $L_{\rm f,0}$ is the length at which the muscle fiber generates maximum tetanic force (see the explanation of how L_{f,O} was estimated in the next section), which allowed us to estimate the relative active and passive forces for a given gape (F_{active}^{Rel} and $F_{passive}^{Rel}$, respectively; Figure 3).

The contribution of tendon strain to muscle segment strain was ignored in this model. The ratio of tendon length (estimated as L_s – $L_{f,occ}$ cos α) to fiber length ranged between 2.0 and 3.1 for all muscles and all species, with a couple of muscle segments that reached 3.5 in Varecia. A muscle with a tendon/fiber length ratio of 3 or lower can be considered having a stiff tendon with a negligible effect on the fiber length-force curve (Zajac, 1989).

2.5 Estimation of optimized muscle model parameters

The musculoskeletal model described above requires muscle architecture parameters such as fiber length and pinnation angle, as well as the estimated changes in muscle segment lengths from the 3D models. Additionally, the musculoskeletal model requires estimating the location of the normalized length-force curve of the masticatory muscles with respect to occlusion (Figure 3). How close the optimum muscle fiber length ($L_{f,0}$) is with respect to the muscle fiber length at occlusion ($L_{f,occ}$) will likely affect the relationship between gape and bite force. If $L_{f,0}$ occurs near occlusion, bite forces would be maximal also near occlusion, and the muscle would operate primarily in the descending limb of the length-force curve as gape increases. In contrast, if $L_{f,0}$ occurs farther from occlusion, bite forces would be maximal at larger gapes, and muscles would operate first in the ascending limb and then in the descending limb of the length-force curve of the muscle as gape increases, therefore, increasing the operating range of the muscle. In the case of the feeding system, we have estimations of the location of the optimal muscle length of the adductor muscles from only a

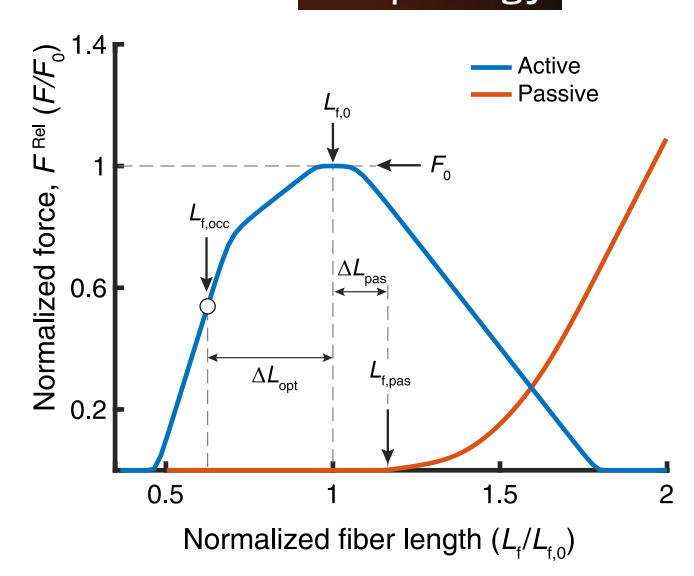


FIGURE 3 Length-force curve and important parameters of the muscle model. The blue and orange lines represent the active and passive components of the length-force curve for a muscle, respectively. $L_{\rm f,0}$ indicates the optimum muscle fiber length at which maximum tetanic active force ($F_{\rm O}$) is generated. $L_{\rm f,occ}$ is the muscle fiber length at occlusion and $L_{\rm f,pas}$ is the muscle fiber length where the passive component of the force becomes non-zero. $\Delta L_{\rm opt}$ is the optimal length offset, the difference in normalized fiber length between $L_{\rm f,0}$ and $L_{\rm f,occ}$. $\Delta L_{\rm pas}$ is the passive length offset, the difference in normalized fiber length between $L_{\rm f,pas}$ and $L_{\rm f,0}$.

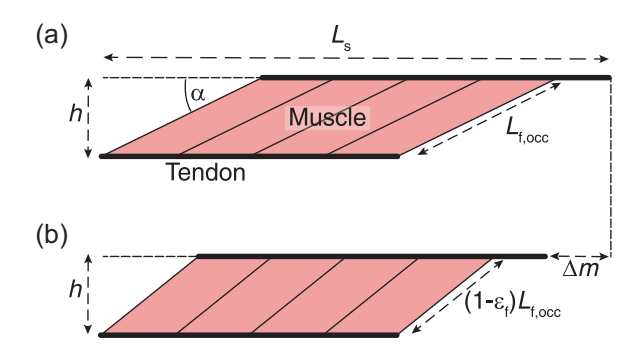


FIGURE 4 Schematic representation of the geometric muscle model used in this study. In this model, the muscle thickness (h) and muscle area remain constant when the muscle goes from its relaxed state (a) to a contracted state (b). L_s , muscle segment length; $L_{f,occ}$, muscle fiber length at occlusion; ϵ_f , muscle fiber strain; α , pinnation angle; Δm , difference in muscle segment length.

couple of primate species, showing differences between species. For example, for *Macaca fascicularis*, its optimum sarcomere lengths occur near to occlusion (Taylor et al., 2019), while for *Callithrix* the optimal sarcomere lengths were estimated at gapes angles ranging from 25 to 55 degrees (Eng et al., 2009). So, without a clear indication of where the location of optimal muscle length is in primates with respect to occlusion, we estimated the optimal length offset ($\Delta L_{\rm opt}$), the normalized difference between $L_{\rm f,0}$ and $L_{\rm f,occ}$ (Figure 3), which best predicted the in vivo bite forces measured for

each species. We also determined $L_{\rm f,pas}$, the normalized fiber length at which the passive forces starts contributing to the total muscle force, by estimating the passive length offset ($\Delta L_{\rm pas}$), the difference between $L_{\rm f,pass}$ and $L_{\rm f,0}$ (Figure 3), considering that this parameter can vary between muscles (Zatsiorsky & Prilutsky, 2012). Finally, also included in the model was a correction factor, cf, that affects the magnitude of the predicted bite force, but it does not change the shape of the bite force-gape relationship. All three parameters ($\Delta L_{\rm opt}$, $\Delta L_{\rm pas}$, and cf), were estimated using "Isqcurvefit," a MATLAB optimization algorithm that searches for the best combination of parameters that minimizes the least-square differences between the predicted bite force values from the in vivo data at different gapes.

To fit the muscle parameters to the experimental bite force data, we first transformed the linear gapes from the bite force data into an angular gape. This was done by simulating different gapes by rotating the mandible in five-degree increments until reaching a 50-degree gape and measuring the linear gape for every tooth for every rotation. We used these data to interpolate the linear gape collected with bite force into an angular gape.

2.6 | Validation of different muscle models

To estimate the effect of different variables on the ability of our musculoskeletal models to predict bite forces with gape, we ran the models for each individual under different muscle architecture parameters but using the same specific 3D bone model.

First, to evaluate the effect of specific muscle architecture parameters on bite force estimates, we ran the models twice for each individual, first using the muscle architecture data generated in this study (i.e., PCSA and fiber lengths) and second using *Eulemur* and *Varecia* muscle architecture measurements published in Perry et al. (2011a; Table 3). Because in this study we did not measure pinnation angles, we used the pinnation angle values from Perry et al. (2011a) in both cases, and because we do not have muscle architecture for *V. variegata*, we used the data from *V. rubra*.

We also created an alternative (MTU) model representing a parallel-fibered muscle. In this model, Equation (4) is modified so that the muscle fiber strain (ϵ_f) is equal to the whole muscle segment strain or MTU strain. This alternative is used to evaluate whether modeling the muscle without muscle architecture complexity was enough to predict the gape-bite force relationship.

To validate whether the geometric muscle models can describe the bite force gape relationship in our sample species, we used the coefficient of determination R^2 as a metric of goodness-of-fit to the experimentally collected in vivo data. R^2 was calculated as 1 – (sum squared of the model, SSM)/(total sum of squares, SST), where SSM is the sum of distance of the data with respect to the predicted value of the model squared, and the SST the sum of the distance of the data from the mean squared. This parameter can be understood as the fraction of the total variance explained by the model. The R^2 -values were also compared to a quadratic polynomial statistical fit of gape

angle versus bite force (Poly model), which is considered here as a reference to the musculoskeletal models.

3 | RESULTS

3.1 | In vivo results—Hypothesis 1

There were no differences between any of the taxa in maximum in vivo bite force (p = .99; Figure 5a). However, maximum in vivo linear

gapes were significantly higher for *V. variegata* compared to *E. flavifrons* ($\chi^2 = 9.0962$, df = 2, p = .01; Figure 5b), and maximum in vivo angular gapes were significantly larger in *V. variegata* compared to *E. flavifrons* and *V. rubra* ($\chi^2 = 9.3233$, df = 2, p = .01; Figure 5c). There were no significant differences in the bite force-gape curve radius of curvature among any of the taxa (p = .29).

Following procedures in Hylander (2013), we measured maximum linear gape at the central incisors as 66.9 mm and maximum linear gape at M_1 as 44.01 mm for one of the V. variegata females in this study during sedation.

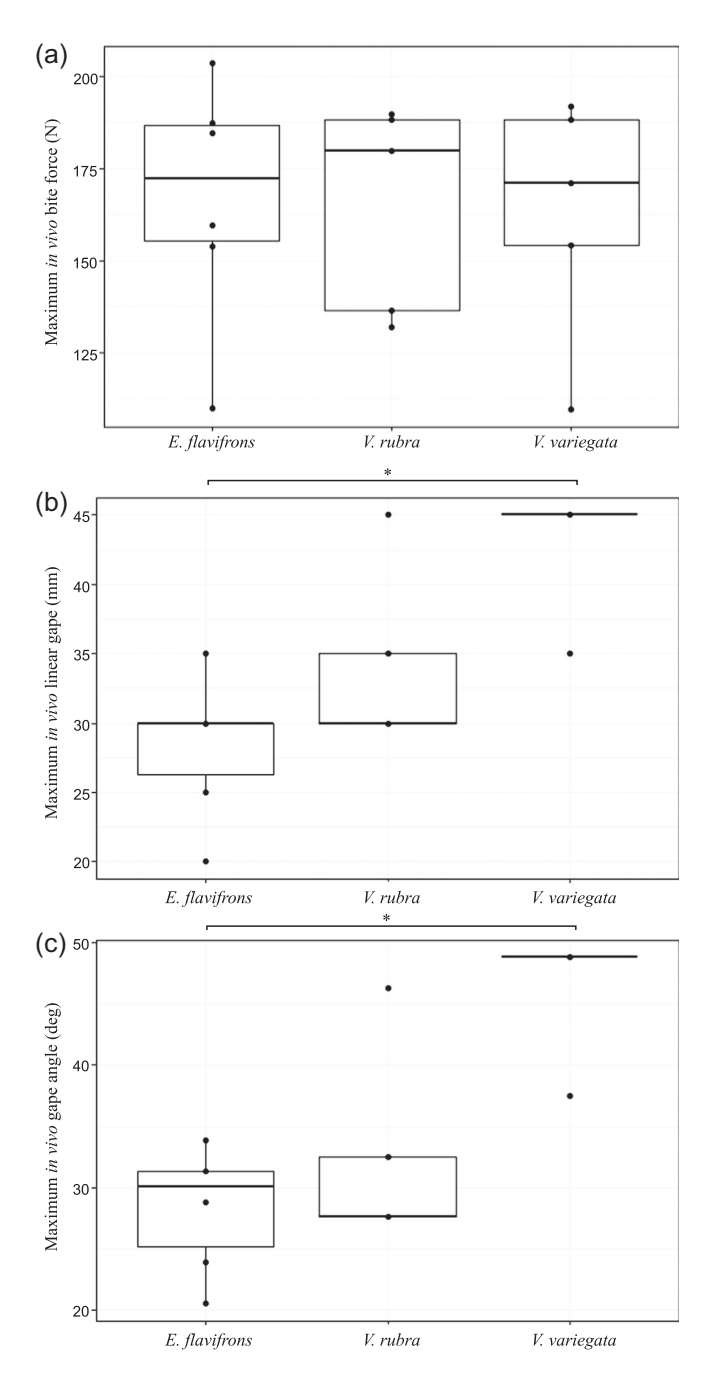


FIGURE 5 Boxplots of maximum recorded in vivo bite force (a), linear gape (b), and angular gape (c). *Varecia variegata* had significantly higher linear and angular gapes compared to *Eulemur* (both p < .03) but none of the taxa differed in bite force (p = .99).

3.1.1 | Effect of gape on bite force-in vivo data

All species showed a curvilinear bite force gape relationship but with varying degrees of variation (R^2 -values for the polynomial fit of 0.5–0.7 for *Eulemur*, 0.4 for *V. rubra*, and 0.28 for *V. variegata*; Figure 6). Peak bite force occurred at gapes between 17 and 25 degrees for all individuals (Table 4).

3.2 | Modeling results—Hypothesis 2

The optimized musculoskeletal model described the shape of the gape-bite force relationship for all individuals (thick black line in Figure 6), although the model tended to overestimate bite forces at large gape angles. The model also predicted the gape angle that produces maximum bite force (optimal gape angle, Table 4). Our

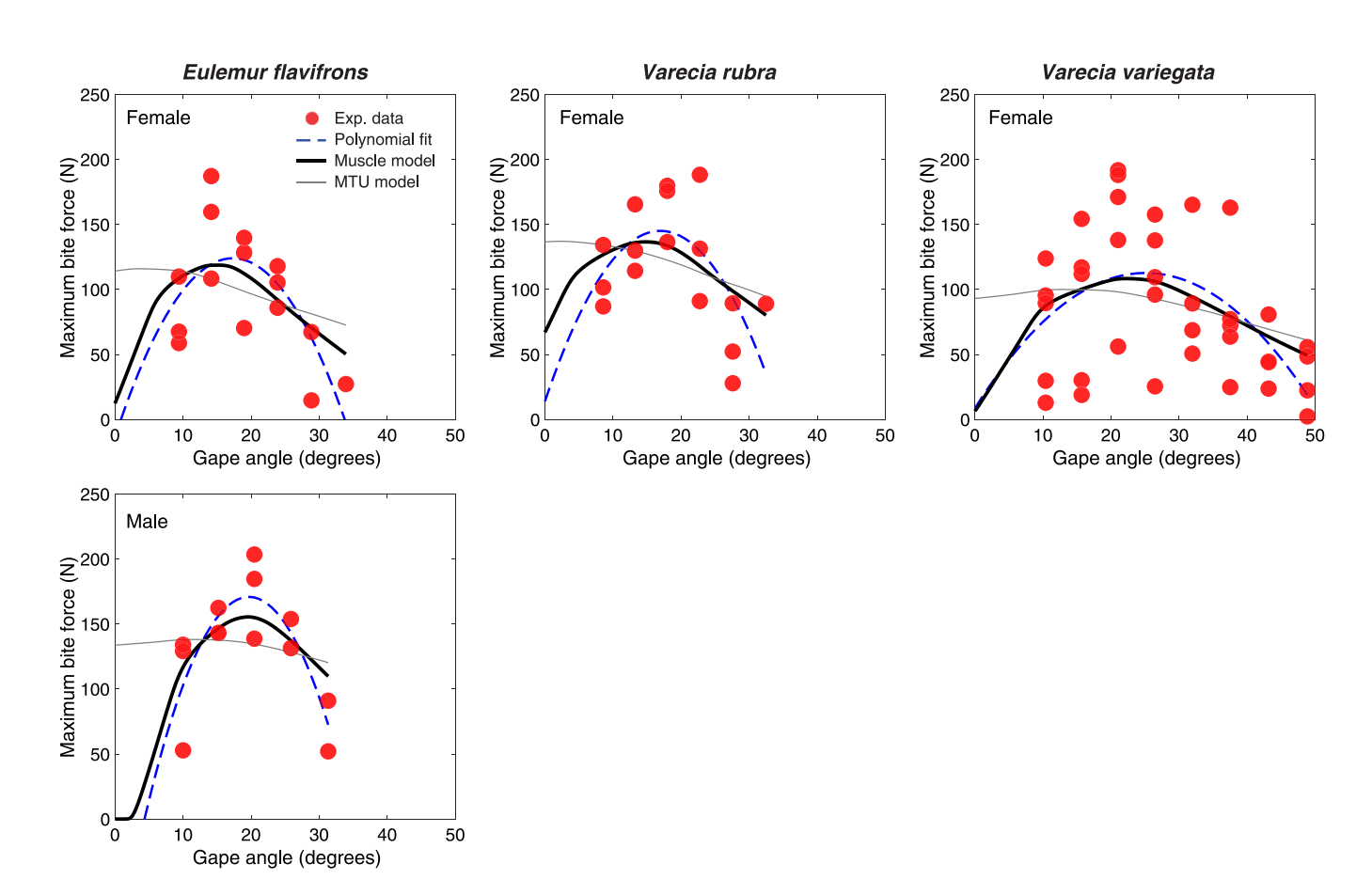


FIGURE 6 Comparison of the experimentally collected bite force data with predicted values from the musculoskeletal model using muscle architecture data from this study. Each point represents the maximum bite force from the in vivo data collected at a given gape angle. The dashed blue line indicates the polynomial fit to the experimental data, representing the general shape of the relationship between gape and bite force. The thick black line represents the predicted bite force for the optimized muscle model and the thin gray line represents the predicted bite force assuming that the muscle is non-pinnate, where the muscle fiber strain corresponds to the MTU strain (MTU model). MTU, muscle-tendon unit.

TABLE 4 Optimized muscle parameters calculated for each species model.

		Optimized model parameters			Optimal ga	pe (degrees)	R ²	R ²	
Species	Sex	$\Delta L_{\rm opt}$	ΔL_{pas}	cf	Poly	Model	Poly	Model	
Eulemur flavifrons	F	0.50	0.83	1.8	17.3	15.1	0.51	0.43	
	М	0.59	0.64	2.6	20.0	19.6	0.67	0.49	
Varecia rubra	F	0.40	0.38	2.3	16.9	14.8	0.40	0.34	
Varecia variegata	F	0.51	0.75	1.8	25.0	22.2	0.28	0.26	

Note: $\Delta L_{\rm opt}$ is the peak length offset, $\Delta L_{\rm pas}$ is the passive length offset, and cf is the correction factor. Optimal gape angle is the gape angle that generates maximal force by the polynomial fit (Poly) and by the muscle model (Model). R^2 indicates the ratio of the variance explained by the polynomial fit (Poly) and by the muscle model (Model).

model slightly underestimated the optimal gape calculated from the polynomial fit, with a difference ranging from -0.4 to -2.8 degrees. To evaluate how well our model described the gape-bite force relationship, we compared the goodness-of-fit of our model to the quadratic polynomial statistical fit. Our model explained 8%-18% less of the total variance than the polynomial fit for *Eulemur*. Visually, the muscle model described the overall shape of the relationship. For *V. rubra*, the muscle model only explained 6% less of the variance than the polynomial fit. However, for *V. variegata*, our muscle model could explain almost as much variance as the polynomial fit, but with a lower fit due to the noisiness of the data.

Our models estimated that peak muscle force does not occur at occlusion but when the muscle fibers are substantially stretched ($\Delta L_{\rm opt}$ >> 0). For *Eulemur*, the values for $\Delta L_{\rm opt}$ ranged from 0.50 to 0.59, while that for *V. rubra* and *V. variegata*, the values were 0.40 and 0.51, respectively. For the passive length offset, all individuals showed a $\Delta L_{\rm pas}$ > 0.64, except for *V. rubra* ($\Delta L_{\rm pas}$ = 0.38). Finally, despite the model being capable of describing well the shape of the bite force-gape relationship, our model consistently underestimated the bite force for a given gape, requiring relatively large correction factors, with the lowest correction factor for *V. variegata* (*cf* = 1.8).

3.2.1 | Effect of variation in muscle architecture parameters on bite force estimation

When comparing our muscle model with the MTU model, which assumes simple, parallel-fibered, muscle architecture, the MTU model does not properly estimate the gape-bite force relationship, showing a very shallow decrease in bite force away from the optimal gape, overestimating bite forces both at small and large gapes (Figure 6). The MTU model also underestimated the optimal gape for all species

(40%–84% decrease in gape angle) and explained only between 10% and 19% of the total variance (Table 5).

When using the muscle architecture parameters from Perry et al. (2011a) instead of the values calculated in this paper, we observe some differences in bite force estimations and muscle model parameters (Table 5). These differences were primarily in the correction factor cf, decreasing by 22%–23% in Eulemur and about 34% in Varecia. In contrast, the location of the optimal fiber length with respect to occlusion ($\Delta L_{\rm opt}$) varied only 2%–3% in Eulemur and 13%–16% in Varecia. Estimation of the optimal gape was also affected, with a 16%–20% increase in gape angle for Eulemur and a 9%–11% decrease in Varecia. Nonetheless, these changes represented differences in gape angles of less than 4 degrees.

3.3 | Differences in the estimated operating range of the jaw adductor muscles—Hypothesis 3

We used the range of observed gapes used in the in vivo data collection to estimate the operating ranges of the jaw adductor muscle fibers at a range of gapes based on our optimized muscle models (Figure 7 and Table 6). For the muscle segment situated closest to the jaw joint, both the superficial masseter and medial pterygoid muscles operate at fiber lengths below the optimum length in all species. The temporalis, however, also operates sometimes above optimum fiber length. For the muscle segments most distally located from the jaw joint, all muscles operate primarily but not exclusively beyond the optimum fiber length. Interestingly, the operating ranges for *Eulemur* and *V. rubra* appear similar, but distinct from the operating ranges of *V. variegata* that tends to show larger operating ranges and more overlap between the proximal and distal muscle segments for the temporalis (Figure 7c).

TABLE 5 Optimized muscle parameters and comparisons for models using different muscle architecture values.

MTU model					Perry et al.'s model						
		Optimized	Optimized model parameters		Optimal gape		Optimize	Optimized model parameters			
Species	Sex	$\Delta L_{\rm opt}$	ΔL_{pas}	cf	(degrees)	R ²	ΔL_{opt}	ΔL_{pas}	cf	(degrees)	R^2
Eulemur flavifrons	F	0.08	0.51	1.6	3.8	0.19	0.49	0.96	1.4	17.4	0.39
		(-84%)	(-39%)	(-11%)	(-75%)	(-56%)	(-2%)	(+16%)	(-22%)	(+16%)	(-9%)
	М	0.20	0.95	2.1	11.7	0.10	0.61	0.58	2.0	23.6	0.47
		(-66%)	(+48%)	(-19%)	(-40%)	(-80%)	(+3%)	(-9%)	(-23%)	(+20%)	(-4%)
Varecia rubra	F	0.08	0.79	2.1	2.3	0.16	0.35	0.70	1.5	13.2	0.31
		(-80%)	(+108%)	(-9%)	(-84%)	(-53%)	(-13%)	(+84%)	(-35%)	(-11%)	(-9%)
Varecia variegata	F	0.20	0.68	1.6	12.8	0.15	0.43	0.70	1.2	20.3	0.23
		(-61%)	(-10%)	(-11%)	(-42%)	(-42%)	(-16%)	(-6%)	(-33%)	(-9%)	(-12%)

Note: The data are presented as the parameter value and, in parenthesis, its percent different from the parameter estimated from the model using the muscle architecture from this paper. The MTU model assumes a parallel-fibered muscle while Perry et al.'s data model uses muscle architecture data from Perry et al. (2011a).

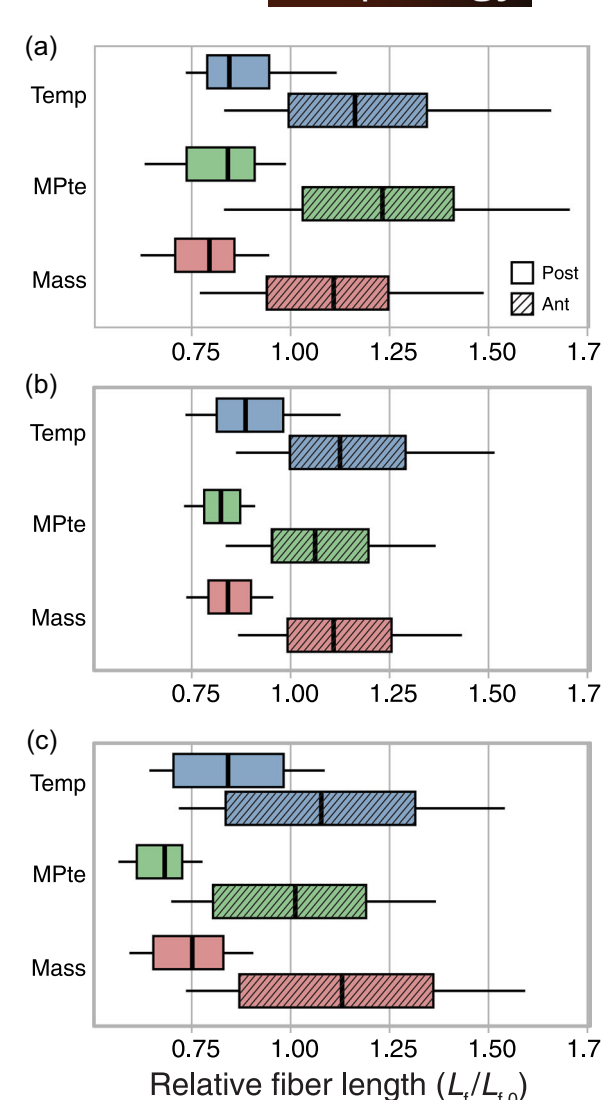


FIGURE 7 Summary of estimated relative muscle fiber lengths during bite force experimental recordings. (a) Data from *Eulemur flavifrons*; (b) *Varecia rubra*; (c) *Varecia variegata*. Each boxplot represents the distribution of estimated fibers strains for the most posterior muscle segment (open boxplots) and for the most anterior muscle segment (shaded boxplots). Blue boxplots represent the temporalis muscle (Temp), green boxplots represent the medial pterygoid muscle (MPte), and the red boxplots represent the superficial masseter muscle (Mass). A relative fiber length of one indicates that the muscle is at its optimal length, while values lower or higher than 1 indicate the muscle is operating in either the ascending limb or the descending limb of the length-tension curve, respectively.

4 | DISCUSSION

Tradeoffs between bite force and gape in the mammalian feeding system have been documented in a number of taxa (Dumont & Herrel, 2003; Herring & Herring, 1974; van Eijden & Turkawski, 2001; Eng et al., 2009; Lindauer et al., 1993; Santana, 2016; Williams et al., 2009), but few studies have addressed these performance factors in primates. This study compared in vivo data capturing changes in bite force with gape in *Eulemur* and *Varecia* with output

from simulated musculoskeletal models of the primate jaw adductors. Our results suggest these lemurids differ in linear and angular gape but not bite force, and musculoskeletal models captured most bite force-gape variation. These results support model validity and their use in estimating bite force-gape relationships in extant and fossil taxa for which in vivo data are not available.

Our data provide the largest reported sample of in vivo bite forces at varying gapes in strepsirrhines, although we acknowledge some limitations of our sample. Male and female E. flavifrons and V. variegata were represented by only two or three animals, and we were only able to collect data from female V. rubra. These samples indicate that we are likely underestimating differences related to sexual dimorphism and interindividual variation; bites collected from a larger number of individuals would most likely expand the in vivo range of bite force and potentially gape. We were not able to build the muscle models using 3D scans from the in vivo sample animals. While this may have reduced the ability of the muscle models to predict in vivo variation, this scenario broadens the applicability of our approach to extant or fossil primates where in vivo data are not available. Simulated muscle models inherently involve a series of assumptions that are detailed in the methods. The models in this manuscript use available data and commonly used values such as muscle specific tension; however, Holmes and Taylor (2021) report that using a single specific tension value can overestimate masseter and temporalis force production up to 44%. Additional in vivo and muscle data specific to these taxa may improve the accuracy of the models.

4.1 | Eulemur and Varecia differ in linear and angular gape, but not bite force

Our results suggested that *Varecia* had larger in vivo linear gapes compared to *Eulemur*, but these genera did not differ in bite force. This result is consistent with data on maximum ingested bite sizes, which indicate that larger gapes in *Varecia* reflect their increased body size and jaw length compared to *Eulemur* (Perry & Hartstone-Rose, 2010). Our in vivo bite force result differs from summed PCSA values for the genera (Perry et al., 2011a), although, we note there are few PCSA differences between the three largest jaw adductors in Perry et al. (2011a) and our PCSA data (Table 3). This means that our in vivo data suggest *Varecia* does not have larger bite force capacities despite their longer jaw lengths and larger body sizes, but we expand upon this finding with the muscle simulation models below.

Here, we consider our in vivo data in the context of available strepsirrhine bite force estimates derived from muscle architecture. In vivo bite forces have not been published for either *Eulemur* or *Varecia*, but a maximum postcanine bite force of 46.09 N was recorded for *Otolemur crassicaudatus* using a similar transducer at a single gape (Hylander, 1977). Our maximum bite forces exceed this value (maximum = 203.46 N; average = 166.46 ± 33.27 N for *E. flavifrons* and maximum = 189.84 N; average = 165.24 ± 28.63 N for *V. rubra*), which is to be expected as *Otolemur* is approximately

Relative muscle fiber length ranges (as % of optimal fiber length) for the most anterior and most posterior segments of the masticatory muscles.

		Relative fibe	Relative fiber length range (%)								
		Posterior se	gment		Anterior segn						
Species	Sex	Mass	MPte	Temp	Mass	MPte	Temp				
Eulemur flavifrons	F	61-90	63-98	73-111	78-153	83-170	83-165				
	М	52-70	55-76	61-105	71-129	74-138	75-146				
Varecia rubra	F	72-88	72-90	72-111	88-152	83-136	85-150				
Varecia variegata	F	58-80	57-78	64-108	73-157	70-137	72-154				

Note: Mass is the masseter, MPte is the medial pterygoid, and Temp is the temporalis.

half the average Eulemur body mass and a third of Varecia. Further, the Otolemur bites were recorded at a single gape that was likely smaller than the optimal muscle fiber length. Postcanine bite force estimates using a combination of muscle architecture data and skeletal measures have been generated for V. rubra at 69.55 N and E. flavifrons at 44.90 N (Perry et al., 2011b). These measures are substantially below our in vivo bite forces, underscoring the need for in vivo data in primates to calibrate muscle and mechanical models.

Despite the importance of gape in relation to bite force as well as primate grooming and display, few studies have examined variation in primate in vivo linear or angular gape (e.g., Hylander, 2013), and the data presented here allow for a rare comparison. Following procedures in Hylander (2013), linear gape in a single V. variegata female ranged from 44.01 to 66.9 mm depending on measurement location on the toothrow. Using the bite force transducer, we recorded a maximum gape of 45 mm in this animal at the premolars suggesting that the bite force transducer used here can capture gapes similar to those measured under sedation. Gape has also been estimated using skeletal proxies, and Fricano and Perry (2019) report linear maximum bony gapes measured between prosthion and infradentale of 73.6-51.7 mm in Varecia and 47.3-45.4 mm in Eulemur. Accounting for differences in measurement, these bony estimates appear to be similar to the in vivo linear gapes presented in this study and from the single Varecia measured during sedation.

The other approach used to measure gape in these taxa, and several other primates, is maximum ingested food size (V_b) (strepsirrhines—Hartstone-Rose & Perry, 2011; Hartstone-Rose et al., 2015; Perry & Hartstone-Rose, 2010, anthropoids-Perry et al., 2015, and gorillas—Paciulli et al., 2020). This method measures the largest volume of food cubes cut by the researcher that an animal will ingest without breaking the food into smaller pieces (Perry & Hartstone-Rose, 2010). The maximum V_b recorded by Perry and Hartstone-Rose (2010) was 27 mm for E. flavifrons and 38 mm for V. rubra. We recorded a maximum in vivo linear gape of 35 mm in E. flavifrons and 45 mm in V. rubra, suggesting that V_b likely underestimates maximum gapes, though this measure may be informative for studies of feeding behavior.

4.2 | Simulated muscle models capture bite force-gape variation

Overall, the simulated muscle model results did not differ from the in vivo bite force-gape data for Varecia and Eulemur, supporting our second hypothesis. Modeled bite force-gape relationships captured the curved shape of the relationship, explained only slightly less variation than a polynomial fit of the in vivo data, and were substantially better at capturing bite force-gape variance compared to simple MTU models. This comparison between in vivo and modeling types is an important validation of muscle simulation models in the primate feeding system.

Musculoskeletal models can provide data on performance factors in the feeding system that are not easily measured in vivo. This includes the gape at which maximum force occurs and the operating range of the jaw adductor muscles. For Eulemur and V. variegata, the fibers of the adductor muscles that produce maximum force are stretched more from occlusion (i.e., higher $\Delta L_{\rm opt}$) in Eulemur and V. variegata than in V. rubra. Interestingly, this difference is not reflected in the optimal gape at which maximal bite force is generated, as indicated by the in vivo data, where optimal gape angle is larger in V. variegata than for V. rubra and Eulemur. We note the V. variegata bite force data were particularly variable compared to the other taxa, which may influence our comparisons between V. variegata and V. rubra (Figure 6). With this consideration, the fiber length operating range in V. variegata was closer to the optimal muscle fiber length than in the other two species (Figure 7c), which suggests the musculoskeletal configuration of the jaw adductor muscles allows the bite force of V. variegata to be relatively less affected by large gapes compared to other species and allows them to use relatively higher forces at large gapes in vivo. This could reflect dietary differences between species, where Varecia feeds primarily on fruits while Eulemur, although mainly frugivorous, has a more varied diet than Varecia (Vasey, 2000). However, dietary ecology is unlikely to explain the differences between V. variegata and V. rubra, as both are primarily frugivorous (Britt, 2000; Rigamonti, 1993). Data generated by muscle simulation models expand upon in vivo measures of bite force and gape and offer additional insight and context into these relationships.

.0974687, 2024, 5, Downloaded wiley.com/doi/10.1002/jmor.21699 by University Of Pennsylvania Library on [19/07/2024]. See the Library for rules of

Interestingly, our muscle simulation models tended to slightly overestimate bite forces at large gapes. This indicates that bite force decreases faster than predicted by our model at large gapes. This may imply that the animals in our study did not apply all available bite force at large gapes, potentially because these large gapes are rarely used during normal behaviors. Joint reaction forces also increasingly vary in magnitude and orientation at large gapes, so the animals may have reduced their bite forces to avoid damaging the temporomandibular joint (e.g., Greaves, 1978; Hylander, 1979; Smith, 1978). Alternatively, this overestimation may indicate a deficit in our model. One possibility is that the generalized muscle length-force curve used in our model does not accurately represent the length dependency of force generation of jaw adductor muscles tested in this study. Considerable variation in the width of normalized length-force relationships has been observed in muscles (Mendoza et al., 2023). Most of the differences in width are between vertebrate and invertebrate muscle, but some variation is present within vertebrate skeletal muscle. Caution must be taken when comparing standardized muscle curves due to differences in methods used between studies, but if some of this variation is real, it could explain the differences between the predicted values from our models and the experimentally recorded bite force data. In any case, in all our optimized models, the passive component is of little or no importance for predicting bite force, which is unlikely to be true. If the passive force component were more important in our model, the overestimation of the bite force at large gapes would be even more pronounced than it is now.

We found differences in bite force estimations depending on muscle architecture input variables. Muscle simulation models were run both using muscle architecture data from Perry et al. (2011a) and architecture data collected for this study (Table 3). These simulations resulted in little variation in the shape of the bite force-gape relationship (e.g., similar $\Delta L_{\rm opt}$ and optimal gape angles) but substantial variation in the magnitude of the estimated bite forces, evidenced by the variation in correction factors (Table 4). This suggests that musculoskeletal models are robust at predicting the relative effect of gape on bite force, but sensitive to architectural estimates of maximal bite forces (Gröning et al., 2013). In our case, the underestimations of bite force using the muscle architecture measured in this paper are due primarily to much lower PCSAs for both Eulemur and Varecia with respect to reported PCSAs from Perry et al. (2011a). PCSA is influenced most heavily by muscle mass and our muscle masses for the three jaw adductors are ~56%-76% of those reported by Perry et al. (2011a; Table 3), with the greatest differences between our Varecia samples. A fair amount of within-species variation (including sexual size dimorphism) has been reported in strepsirrhines (e.g., Perry et al., 2011a; Taylor et al., 2024) and anthropoid primate chewing muscles (e.g., Terhune et al., 2015, 2018). Thus, differences between our estimates could be the result of normal intraspecific variation. Additional non-mutually exclusive factors could be the inclusion of only captive specimens in our estimate

compared to the combination of captive and wild *Varecia* specimens in Perry et al. (2011a), differences between our samples in adult status and age-related muscle loss (Colman et al., 2005), differences in muscle definitions, and/or differences in measurement techniques (but see Taylor et al., 2024).

Skeletal muscle fibers have been shown to have substantial intra- and interspecific variation in the ranges of sarcomere length at which they operate (see Burkholder & Lieber, 2001 for a survey of sarcomere-length operating length ranges for limb and jaw muscle within vertebrates). The estimated operating ranges of the masticatory muscle fibers in our study show comparable ranges to those observed in other mammalian species. The minimum relative fiber lengths (as a percentage of $L_{f,0}$) estimated in our species range from 52% to 73% for anterior muscle segments and from 70% to 88% for posterior muscle segments, which are not dissimilar from the 66%-95% range of minimum sarcomeres lengths reported in a few primate species (Eng et al., 2009; Taylor et al., 2019) and from the 74%-93% range of minimum sarcomeres lengths reported in non-primate species (Burkholder Lieber, 2001). The maximum relative fiber lengths estimated in our study were 70%-111% for anterior muscle segments and 129%-170% for posterior muscle segments. These are higher than upper length ranges observed in primate (83%-160%) and in nonprimate species (95%-126%), as well as for the reported upper range for non-masticatory muscles (Burkholder & Lieber, 2001). An upper value of 189% has been reported for the human masseter (van Eijden & Raadsheer, 1992), but this value was obtained from models, and it is likely to be an overestimation (Taylor et al., 2019). A possible explanation of the high upper range values in fiber length observed in this study may be our assumption that muscle architecture parameters are constant across muscle segments, with anterior and posterior muscle segments having the same fiber length. Under these conditions, anterior muscle segments are expected to stretch more than posterior muscle segments. However, some primates show substantial intramuscular variation in fiber length, though the pattern of variation is muscle dependent. For example, both Macaca fascicularis and M. mulatta have longer muscle fibers in the anterior compared to the posterior portion of the superficial masseter, but show the opposite pattern for the temporalis i.e., shorter muscle fibers in the anterior compared to the posterior portion of the muscle (Taylor et al., 2019; Terhune et al., 2015). Additional architecture data are needed to compare within-muscle variation in fiber length in Eulemur and Varecia and in other primates.

5 | CONCLUSIONS

This study provides validation for bite force-gape musculoskeletal modeling in the primate feeding system. These models build on the foundational work of Herring and Herring (1974) providing important information on how gape affects relative bite force generation and peak gape angles, which can inform dietary adaptations in primates and selection for functional demands on primate craniofacial morphology. For example, frugivorous primates should have larger optimal gapes than folivores, and expanding these approaches to a broader selection of primates can inform the role of selection for optimal gapes within the functional design of the feeding system. Our results also underscore the necessity of collecting more in vivo data on bite force and gape to provide benchmarks for examining functional performance of the feeding system and in musculoskeletal modeling.

AUTHOR CONTRIBUTIONS

Conceptualization: Myra F. Laird, Jose Iriarte-Diaz. Investigation: Myra F. Laird, Taylor A. Polvadore, Gabrielle A. Hirschkorn, Julie C. McKinney, Claire E. Terhune, Jose Iriarte-Diaz. Resources: Myra F. Laird, Taylor A. Polvadore, Gabrielle A. Hirschkorn, Julie C. McKinney, Callum F. Ross, Andrea B. Taylor, Claire E. Terhune, Jose Iriarte-Diaz. Visualization: Myra F. Laird, Jose Iriarte-Diaz. Methodology: Myra F. Laird, Jose Iriarte-Diaz. Formal analysis: Myra F. Laird, Jose Iriarte-Diaz. Writing – original draft preparation: Myra F. Laird, Jose Iriarte-Diaz. Writing – review & editing: Myra F. Laird, Taylor A. Polvadore, Gabrielle A. Hirschkorn, Julie C. McKinney, Callum F. Ross, Andrea B. Taylor, Claire E. Terhune, Jose Iriarte-Diaz. Funding acquisition: Myra F. Laird, Claire E. Terhune, Andrea B. Taylor.

ACKNOWLEDGMENTS

Funding for this project was generously provided by the National Science Foundation (BCS-1945771, BCS-1944915, BCS-1945283, BCS-1945767, BCS 0924592; 0452160) and the University of Southern California Zumberge Award. We thank Elle Fricano for sharing her gape data. Special thanks to Kay Welser, Erin Ehmke, Chris Wall, and DLC caretakers for their assistance in data collection. This is Duke Lemur Center publication #1588.

DATA AVAILABILITY STATEMENT

The data that support the findings of this study are available from the corresponding author upon reasonable request.

ORCID

Myra F. Laird http://orcid.org/0000-0002-8636-0407

Taylor A. Polvadore http://orcid.org/0000-0002-3458-6682

Jose Iriarte-Diaz http://orcid.org/0000-0003-3566-247X

REFERENCES

- Aguirre, L. F., Herrel, A., Van Damme, R., & Matthysen, E. (2003). The implications of food hardness for diet in bats. *Functional Ecology*, 17(2), 201–212.
- Anapol, F., & Herring, S. W. (1989). Length-tension relationships of masseter and digastric muscles of miniature swine during ontogeny. *Journal of Experimental Biology*, 143(1), 1–16.
- Anderson, F. C., & Pandy, M. G. (2003). Individual muscle contributions to support in normal walking. *Gait & Posture*, 17(2), 159–169.

- Antón, S. C. (1999). Macaque masseter muscle: Internal architecture, fiber length and cross-sectional area. *International Journal of Primatology*, 20, 441–462.
- Antón, S. C. (2000). Macaque pterygoid muscles: Internal architecture, fiber length, and cross-sectional area. *International Journal of Primatology*, 21, 131–156.
- Azizi, E., & Deslauriers, A. R. (2014). Regional heterogeneity in muscle fiber strain: The role of fiber architecture. Frontiers in Physiology, 5, 103613.
- Biewener, A. A., Wakeling, J. M., Lee, S. S., & Arnold, A. S. (2014). Validation of hill-type muscle models in relation to neuromuscular recruitment and force-velocity properties: Predicting patterns of in vivo muscle force. *Integrative and Comparative Biology*, 54(6), 1072-1083.
- Britt, A. (2000). Diet and feeding behaviour of the black-and-white ruffed lemur (*Varecia variegata variegata*) in the Betampona Reserve, eastern Madagascar. *Folia Primatologica*, 71(3), 133–141.
- Burkholder, T. J., & Lieber, R. L. (2001). Sarcomere length operating range of vertebrate muscles during movement. *Journal of Experimental Biology*, 204(9), 1529–1536.
- Charles, J., Kissane, R., Hoehfurtner, T., & Bates, K. T. (2022). From fibre to function: Are we accurately representing muscle architecture and performance? *Biological Reviews*, *97*(4), 1640–1676.
- Chazeau, C., Marchal, J., Hackert, R., Perret, M., & Herrel, A. (2013). Proximate determinants of bite force capacity in the mouse lemur. *Journal of Zoology*, 290(1), 42–48.
- Colman, R. J., McKiernan, S. H., Aiken, J. M., & Weindruch, R. (2005). Muscle mass loss in Rhesus monkeys: Age of onset. Experimental Gerontology, 40, 573–581.
- Curtis, N., Kupczik, K., O'higgins, P., Moazen, M., & Fagan, M. (2008).Predicting skull loading: Applying multibody dynamics analysis to a macaque skull. *The Anatomical Record*, 291(5), 491–501.
- Dechow, P. C., & Carlson, D. S. (1983). A method of bite force measurement in primates. *Journal of Biomechanics*, 16(10), 797–802.
- Dechow, P. C., & Carlson, D. S. (1990). Occlusal force and craniofacial biomechanics during growth in rhesus monkeys. American Journal of Physical Anthropology, 83(2), 219–237.
- Delp, S. L., Anderson, F. C., Arnold, A. S., Loan, P., Habib, A., John, C. T., Guendelman, E., & Thelen, D. G. (2007). OpenSim: Open-source software to create and analyze dynamic simulations of movement. *IEEE Transactions on Biomedical Engineering*, 54(11), 1940–1950.
- Dick, T. J. M., & Wakeling, J. M. (2018). Geometric models to explore mechanisms of dynamic shape change in skeletal muscle. Royal Society Open Science, 5(5), 172371.
- Dickinson, E., Pastor, F., Santana, S. E., & Hartstone-Rose, A. (2022). Functional and ecological correlates of the primate jaw abductors. *The Anatomical Record*, 305(5), 1245–1263.
- Dumont, E. R., & Herrel, A. (2003). The effects of gape angle and bite point on bite force in bats. *Journal of Experimental Biology*, 206(13), 2117–2123.
- Edmonds, H. M., & Glowacka, H. (2020). The ontogeny of maximum bite force in humans. *Journal of Anatomy*, 237(3), 529-542.
- van Eijden, T. M. G. J., & Raadsheer, M. C. (1992). Heterogeneity of fiber and sarcomere length in the human masseter muscle. *The Anatomical Record*, 232, 78–84.
- van Eijden, T. M., & Turkawski, S. J. (2001). Morphology and physiology of masticatory muscle motor units. *Critical Reviews in Oral Biology and Medicine*, 12(1), 76–91. https://doi.org/10.1177/1045441101012 0010601
- Eng, C. M., Ward, S. R., Vinyard, C. J., & Taylor, A. B. (2009). The morphology of the masticatory apparatus facilitates muscle force production at wide jaw gapes in tree-gouging common marmosets (Callithrix jacchus). Journal of Experimental Biology, 212(24), 4040–4055.

- Fricano, E. E. I., & Perry, J. M. G. (2019). Maximum bony gape in primates. The Anatomical Record, 302(2), 215-225.
- Gans, C., & Bock, W. J. (1965). The functional significance of muscle architecture: A theoretical analysis. Ergebnisse der Anatomie und Entwicklungsgeschichte, 38, 115-142.
- Greaves, W. S. (1978). The jaw lever system in ungulates: A new model. Journal of Zoology, 184(2), 271–285.
- Gröning, F., Jones, M. E. H., Curtis, N., Herrel, A., O'Higgins, P., Evans, S. E., & Fagan, M. J. (2013). The importance of accurate muscle modelling for biomechanical analyses: A case study with a lizard skull. Journal of the Royal Society Interface, 10(84), 20130216.
- Hartstone-Rose, A., & Perry, J. M. G. (2011). Intraspecific variation in maximum ingested food size and body mass in Varecia rubra and Propithecus coquereli. Anatomy Research International, 2011, 1-8.
- Hartstone-Rose, A., Parkinson, J. A., Criste, T., & Perry, J. M. G. (2015). Comparing apples and oranges-The influence of food mechanical properties on ingestive bite sizes in lemurs. American Journal of Physical Anthropology, 157(3), 513-518.
- Herrel, A., Damme, R. V., Vanhooydonck, B., & Vree, F. D. (2001). The implications of bite performance for diet in two species of lacertid lizards. Canadian Journal of Zoology, 79(4), 662-670.
- Herrel, A., Huyghe, K., Vanhooydonck, B., Backeljau, T., Breugelmans, K., Grbac, I., Van Damme, R., & Irschick, D. J. (2008). Rapid large-scale evolutionary divergence in morphology and performance associated with exploitation of a different dietary resource. Proceedings of the National Academy of Sciences, 105(12), 4792-4795,
- Herrel, A., Podos, J., Huber, S. K., & Hendry, A. P. (2005). Bite performance and morphology in a population of Darwin's finches: Implications for the evolution of beak shape. Functional Ecology, 19(1), 43-48,
- Herrel, A., Spithoven, L., Van Damme, R., & De Vree, F. (1999). Sexual dimorphism of head size in Gallotia galloti: Testing the niche divergence hypothesis by functional analyses. Functional Ecology, 13(3), 289-297.
- Herrel, A., Vanhooydonck, B., & Van Damme, R. (2004). Omnivory in lacertid lizards: Adaptive evolution or constraint? Journal of Evolutionary Biology, 17(5), 974-984.
- Herring, S. W., & Herring, S. E. (1974). The superficial masseter and gape in mammals. The American Naturalist, 108(962), 561-576.
- Hill, A. V. (1938). The heat of shortening and the dynamic constants of muscle. Proceedings of the Royal Society of London. Series B-Biological Sciences, 126(843), 136-195.
- Hill, A. V. (1950). The dimensions of animals and their muscular dynamics. Science Progress, 38(150), 209-230.
- Holmes, M., & Taylor, A. B. (2021). The influence of jaw-muscle fibre-type phenotypes on estimating maximum muscle and bite forces in primates. Interface Focus, 11(5), 20210009.
- Hylander, W. L. (1975). The human mandible: Lever or link? American Journal of Physical Anthropology, 43(2), 227-242.
- Hylander, W. L. (1977). In vivo bone strain in the mandible of Galago crassicaudatus. American Journal of Physical Anthropology, 46(2), 309-326.
- Hylander, W. L. (1979). Mandibular function in Galago crassicaudatus and Macaca fascicularis: An in vivo approach to stress analysis of the mandible. Journal of Morphology, 159(2), 253-296.
- Hylander, W. L. (2013). Functional links between canine height and jaw gape in catarrhines with special reference to early hominins. American Journal of Physical Anthropology, 150(2), 247-259.
- van Ingen Schenau, G. J., Bobbert, M. F., Ettema, G. J., de Graaf, J. B., & Huijing, P. A. (1988). A simulation of rat EDL force output based on intrinsic muscle properties. Journal of Biomechanics, 21, 815-824.

- Iriarte-Diaz, J., Terhune, C. E., Taylor, A. B., & Ross, C. F. (2017). Functional correlates of the position of the axis of rotation of the mandible during chewing in non-human primates. Zoology, 124, 106-118.
- Koolstra, J. H., & Van Eijden, T. M. G. J. (2001). A method to predict muscle control in the kinematically and mechanically indeterminate human masticatory system. Journal of Biomechanics, 34(9), 1179-1188.
- Laird, M. F., Granatosky, M. C., Taylor, A. B., & Ross, C. F. (2020). Muscle architecture dynamics modulate performance of the superficial anterior temporalis muscle during chewing in capuchins. Scientific Reports, 10(1), 6410.
- Laird, M. F., Iriarte-Diaz, J., Byron, C. D., Granatosky, M. C., Taylor, A. B., & Ross, C. F. (2023a). Gape drives regional variation in temporalis architectural dynamics in tufted capuchins. Philosophical Transactions of the Royal Society B, 378(1891), 20220550.
- Laird, M. F., Kanno, C. M., Yoakum, C. B., Fogaça, M. D., Taylor, A. B., Ross, C. F., & de Oliveira, J. A. (2023b). Ontogenetic changes in bite force and gape in tufted capuchins. Journal of Experimental Biology, 226(15), jeb245972.
- Lee, S. S., de Boef Miara, M., Arnold, A. S., Biewener, A. A., & Wakeling, J. M. (2013). Accuracy of gastrocnemius forces in walking and running goats predicted by one-element and two-element Hilltype models. Journal of Biomechanics, 43, 2288-2295.
- Lieber, R. L. (2022). Can we just forget about pennation angle? Journal of Biomechanics, 132, 110954.
- Lindauer, S. J., Gay, T., & Rendell, J. (1993). Effect of jaw opening on masticatory muscle EMG-force characteristics. Journal of Dental Research, 72(1), 51-55.
- Mendoza, E., Moen, D. S., & Holt, N. C. (2023). The importance of comparative physiology: Mechanisms, diversity and adaptation in skeletal muscle physiology and mechanics. Journal of Experimental Biology, 226(1), jeb245158.
- Millard, M., Uchida, T., Seth, A., & Delp, S. L. (2013). Flexing computational muscle: Modeling and simulation of musculotendon dynamics. Journal of Biomechanical Engineering, 135(2), 021005.
- Murphy, R., & Beardsley, A. (1974). Mechanical properties of the cat soleus muscle in situ. American Journal of Physiology-Legacy Content, 227, 1008-1013,
- Paciulli, L. M., Leischner, C., Lane, B. A., McCaughey, M., Guertin, E., Davis, J., Eberth, J. F., & Hartstone-Rose, A. (2020). Brief communication: Maximum ingested bite size in captive western lowland gorillas (Gorilla gorilla). American Journal of Physical Anthropology, 171(4), 725-732.
- Perreault, E. J., Heckman, C. J., & Sandercock, T. G. (2003). Hill muscle model errors during movement are greatest within the physiologically relevant range of motor unit firing rates. Journal of Biomechanics, 36, 211-218.
- Perry, J. M., Hartstone-Rose, A., & Wall, C. E. (2011a). The jaw adductors of strepsirrhines in relation to body size, diet, and ingested food size. The Anatomical Record, 294(4), 712-728.
- Perry, J. M., Hartstone-Rose, A., & Logan, R. L. (2011b). The jaw adductor resultant and estimated bite force in primates. Anatomy Research International, 2011, 929848.
- Perry, J. M. G., Bastian, M. L., St Clair, E., & Hartstone-Rose, A. (2015). Maximum ingested food size in captive anthropoids. American Journal of Physical Anthropology, 158(1), 92-104.
- Perry, J. M. G., & Hartstone-Rose, A. (2010). Maximum ingested food size in captive strepsirrhine primates: Scaling and the effects of diet. American Journal of Physical Anthropology, 142(4), 625-635.
- Peterson, M. D., Pistilli, E., Haff, G. G., Hoffman, E. P., & Gordon, P. M. (2011). Progression of volume load and muscular adaptation during resistance exercise. European Journal of Applied Physiology, 111, 1063-1071.

- Powell, P. L., Roy, R. R., Kanim, P., Bello, M. A., & Edgerton, V. R. (1984).
 Predictability of skeletal muscle tension from architectural determinations in guinea pig hindlimbs. *Journal of Applied Physiology*, 57(6), 1715–1721
- R Core Team. (2023). R: A language and environment for statistical computing. R Foundation for Statistical Computing. https://www.R-project.org/
- Radinsky, L. B. (1981). Evolution of skull shape in carnivores: 2. Additional modern carnivores. *Biological Journal of the Linnean Society*, 16(4), 337–355.
- Rigamonti, M. M. (1993). Home range and diet in red ruffed lemurs (*Varecia variegata rubra*) on the Masoala Peninsula, Madagascar. In P. M. Kappeler & J. U. Ganzhorn, (eds.), *Lemur social systems and their ecological basis* (pp. 25–39). Springer US In.
- Ross, C. F., Porro, L. B., Herrel, A., Evans, S. E., & Fagan, M. J. (2018). Bite force and cranial bone strain in four species of lizards. *Journal of Experimental Biology*, 221, 1–13.
- Ross, C. F., Reed, D. A., Washington, R. L., Eckhardt, A., Anapol, F., & Shahnoor, N. (2009). Scaling of chew cycle duration in primates. American Journal of Physical Anthropology, 138(1), 30–44.
- Sandercock, T. G., & Heckman, C. J. (1997). Force from cat soleus muscle during imposed locomotor-like movements: Experimental data versus Hill-type model predictions. *Journal of Neurophysiology*, 77, 1538–1552.
- Santana, S. E. (2016). Quantifying the effect of gape and morphology on bite force: Biomechanical modelling andin vivomeasurements in bats. *Functional Ecology*, 30(4), 557–565.
- Shi, J., Curtis, N., Fitton, L. C., O'Higgins, P., & Fagan, M. J. (2012). Developing a musculoskeletal model of the primate skull: Predicting muscle activations, bite force, and joint reaction forces using multibody dynamics analysis and advanced optimisation methods. *Journal of Theoretical Biology*, 310, 21–30.
- Smith, R. J. (1978). Mandibular biomechanics and temporomandibular joint function in primates. American Journal of Physical Anthropology, 49, 341–349.
- Smith, R. J. (1984). Comparative functional morphology of maximum mandibular opening (gape) in primates. In D. J. Chivers, B. A. Wood & A. Bilsborough, (Eds), Food acquisition and processing in primates (pp. 231–255). Springer US In.
- Spencer, M. A. (1998). Force production in the primate masticatory system: electromyographic tests of biomechanical hypotheses. *Journal of Human Evolution*, 34(1), 25–54.
- Spencer, M. A. (1999). Constraints on masticatory system evolution in anthropoid primates. American Journal of Physical Anthropology, 108(4), 483–506.
- Taverne, M., Watson, P. J., Dutel, H., Boistel, R., Lisicic, D., Tadic, Z., Fabre, A. C., Fagan, M. J., & Herrel, A. (2023). Formfunction relationships underlie rapid dietary changes in a lizard. Proceedings of the Royal Society B: Biological Sciences, 290(2000), 20230582.
- Taylor, A. B., Eng, C. M., Anapol, F. C., & Vinyard, C. J. (2009). The functional significance of jaw-muscle fiber architecture in treegouging marmosets. In The Smallest Anthropoids: The Marmoset/ Callimico Radiation (pp. 381-394).
- Taylor, A. B., Terhune, C. E., Ross, C. F., & Vinyard, C. J. (2024). The impact of measurement technique and sampling on estimates of skeletal muscle fibre architecture. *Anatomical Record*, 1–14.
- Taylor, A. B., Terhune, C. E., & Vinyard, C. J. (2019). The influence of masseter and temporalis sarcomere length operating ranges as determined by laser diffraction on architectural estimates of muscle force and excursion in macaques (*Macaca fascicularis* and *Macaca mulatta*). Archives of Oral Biology, 105, 35-45.
- Taylor, A. B., & Vinyard, C. J. (2009). Jaw-muscle fiber architecture in tufted capuchins favors generating relatively large muscle forces

- without compromising jaw gape. *Journal of Human Evolution*, 57(6), 710-720.
- Terhune, C. E., Hylander, W. L., Vinyard, C. J., & Taylor, A. B. (2015). Jaw-muscle architecture and mandibular morphology influence relative maximum jaw gapes in the sexually dimorphic *Macaca fascicularis*. *Journal of Human Evolution*, 82, 145–158.
- Thelen, D. G. (2003). Adjustment of muscle mechanics model parameters to simulate dynamic contractions in older adults. *Journal of Biomechanical Engineering*, 125(1), 70–77.
- Thomas, P., Pouydebat, E., Hardy, I., Aujard, F., Ross, C. F., & Herrel, A. (2015). Sexual dimorphism in bite force in the grey mouse lemur. *Journal of Zoology*, 296(2), 133–138.
- Thompson, E. N., Biknevicius, A. R., & German, R. Z. (2003). Ontogeny of feeding function in the gray short-tailed opossum *Monodelphis domestica*: Empirical support for the constrained model of jaw biomechanics. *Journal of Experimental Biology*, 206(5), 923–932.
- Turkawski, S., & Eijden, T. (2001). Mechanical properties of single motor units in the rabbit masseter muscle as a function of jaw position. Experimental Brain Research, 138, 153-162.
- Vasey, N. (2000). Niche separation in Varecia variegata rubra and Eulemur fulvus albifrons: I. Interspecific patterns. American Journal of Physical Anthropology, 112(3), 411–431.
- Verwaijen, D., Van Damme, R., & Herrel, A. (2002). Relationships between head size, bite force, prey handling efficiency and diet in two sympatric lacertid lizards. *Functional Ecology*, 16(6), 842–850.
- Vinyard, C. J., Wall, C. E., Williams, S. H., & Hylander, W. L. (2003). Comparative functional analysis of skull morphology of tree-gouging primates. American Journal of Physical Anthropology, 120(2), 153–170.
- Vinyard, C. J., Wall, C. E., Williams, S. H., Mork, A. L., Armfield, B. A., Melo, L. C. D. O., & Hylander, W. L. (2009). The evolutionary morphology of tree gouging in marmosets. In The Smallest Anthropoids: The Marmoset/Callimico Radiation (pp. 395-409).
- Wakeling, J. M., Lee, S. S. M., Arnold, A. S., de Boef Miara, M., & Biewener, A. A. (2012). A muscle's force depends on the recruitment patterns of its fibers. *Annals of Biomedical Engineering*, 40, 1708–1720.
- Wall, C. E., Briggs, M. M., Huq, E., Hylander, W. L., & Schachat, F. (2013). Regional variation in IIM myosin heavy chain expression in the temporalis muscle of female and male baboons (*Papio anubis*). Archives of Oral Biology, 58(4), 435–443.
- Wickham, H. (2016). ggplot2: Elegant Graphics for Data Analysis. Springer-Verlag.
- Wickham, H., & Bryan, J. (2022). readxl: Read Excel Files. R package version 1.4.0.
- Williams, S. H., Peiffer, E., & Ford, S. (2009). Gape and bite force in the rodents Onychomys leucogaster and Peromyscus maniculatus: Does jaw-muscle anatomy predict performance? Journal of Morphology, 270(11), 1338–1347.
- Wright, B. (2005). Craniodental biomechanics and dietary toughness in the genus. *Journal of Human Evolution*, 48(5), 473–492.
- Xiao, N. (2018). ggsci: Scientific Journal and Sci-Fi Themed Color Palettes for 'ggplot2'. R package version 2.9.
- Xu, W. L., Bronlund, J. E., Potgieter, J., Foster, K. D., Röhrle, O., Pullan, A. J., & Kieser, J. A. (2008). Review of the human masticatory system and masticatory robotics. *Mechanism and Machine Theory*, 43(11), 1353–1375.
- Zablocki Thomas, P. B., Karanewsky, C. J., Pendleton, J. L., Aujard, F., Pouydebat, E., & Herrel, A. (2018). Drivers of *in vivo* bite performance in wild brown mouse lemurs and a comparison with the grey mouse lemur. *Journal of Zoology*, 305(3), 180–187.
- Zajac, F. E. (1989). Muscle and tendon: Properties, models, scaling, and application to biomechanics and motor control. *Critical Reviews in Biomedical Engineering*, 17, 359–411.
- Zatsiorsky, V. M., & Prilutsky, B. I. (2012). *Biomechanics of skeletal muscles*. (Vol. 47, Issue 2) Human Kinetics Publishers.

de Zee, M., Dalstra, M., Cattaneo, P. M., Rasmussen, J., Svensson, P., & Melsen, B. (2007). Validation of a musculo-skeletal model of the mandible and its application to mandibular distraction osteogenesis. *Journal of Biomechanics*, 40(6), 1192–1201.

SUPPORTING INFORMATION

Additional supporting information can be found online in the Supporting Information section at the end of this article.

How to cite this article: Laird, M. F., Polvadore, T. A., Hirschkorn, G. A., McKinney, J. C., Ross, C. F., Taylor, A. B., Terhune, C. E., & Iriarte-Diaz, J. (2024). Tradeoffs between bite force and gape in *Eulemur* and *Varecia*. *Journal of Morphology*, 285, e21699.

https://doi.org/10.1002/jmor.21699